Annual Application and Evaluation of the Online Coupled WRF-CMAQ System over North America under AQMEII Phase 2

Christian Hogrefe[1,*], George Pouliot[1], David Wong[1], Alfreida Torian[1], Shawn Roselle[1], Jonathan Pleim[1], and Rohit Mathur[1]

[1]Atmospheric Modeling and Analysis Division, National Exposure Research Laboratory, Office of Research and Development, U.S. Environmental Protection Agency

[*]Corresponding author contact information: Christian Hogrefe, Atmospheric Modeling and Analysis Division, MD E243-04, U.S. Environmental Protection Agency, Research Triangle Park, NC 27711, USA; Email: hogrefe.christian@epa.gov

Manuscript Submitted to Atmospheric Environment, May 29, 2014

Abstract

We present an application of the online coupled Weather Research and Forecasting – Community Multiscale Air Quality (WRF-CMAQ) modeling system to two annual simulations over North America performed under Phase 2 of the Air Quality Model Evaluation International Initiative (AQMEII). Operational evaluation shows that model performance is comparable to earlier annual applications of the uncoupled WRF/CMAQ modeling system Results also indicate that factors such as changes in the underlying emissions inventory and chemical boundary conditions likely exerted a larger influence on overall model performance than feedback effects. A comparison of the simulated Aerosol Optical Depth (AOD) against observations reveals a tendency toward underprediction in all seasons despite a general overprediction of $PM_{2.5}$ during wintertime. Summertime sensitivity simulations without feedback effects are used to quantify the average impact of the simulated direct feedback effect on temperature, PBL heights, ozone and $PM_{2.5}$ concentrations. Model results for 2006 and 2010 are analyzed to compare modeled changes between these years to those seen in observations. The results for summertime average daily maximum 8-hr ozone showed that the model tends to underestimate the observed decrease in concentrations. The results for total and speciated $PM_{2.5}$ vary between seasons, networks and species, but the WRF-CMAQ simulations do capture the substantial decreases in observed $PM_{2.5}$ concentrations in summer and fall. These 2010-2006 $PM_{2.5}$ decreases result in simulated increases of summer mean clear-sky shortwave radiation between 5 and 10 W/m^2. The WRF-CMAQ configuration without direct feedback effects simulates smaller changes in summertime $PM_{2.5}$ concentrations, indicating that the direct feedback effect enhances the air quality benefits arising from emission controls and that coupled modeling systems are necessary to quantify such feedback effects.

Highlights

- Coupled WRF-CMAQ modeling system applied and evaluated for two annual simulations under AQMEII Phase 2
- Model performance comparable to earlier applications of the uncoupled modeling system
- The coupled modeling system captures the substantial reductions in summer and fall $PM_{2.5}$ concentrations between 2006 and 2010 and allows the quantification of the radiative impacts of these changes

Keywords:

WRF-CMAQ coupled model, AQMEII, direct feedbacks, dynamic evaluation

1.Introduction

Regional-scale air quality modeling systems are frequently used for air quality forecasting and planning purposes and typically consist of a meteorological component and a chemical transport component. Traditionally, the meteorological component is applied first and the resulting output fields are used as input to the chemical transport modeling component. Such an approach is often referred to as "offline" or "uncoupled" air quality modeling. In contrast, "online" or "coupled" modeling systems imply that the meteorological and chemical transport components of the modeling system are applied simultaneously and optionally include mechanisms through which the chemical transport component can provide feedbacks to the meteorological component (Grell et al., 2005; Zhang, 2008; Baklanov et al., 2014). The Community Multiscale Air Quality (CMAQ) modeling system developed by the U.S. Environmental Protection Agency (U.S. EPA) has historically been an "uncoupled" model (Byun and Schere, 2006) but has recently been enhanced to offer users the option of "coupled" applications (Wong et al., 2012) with the Weather Research and Forecasting (WRF) model (Skamarock et al., 2008). In this study, we present the first annual application and evaluation of this coupled WRF-CMAQ modeling system. These simulations were performed for 2006 and 2010 in the context of the second phase of the Air Quality Model Evaluation International Initiative (AQMEII) and covered the entire United States. The current study has several objectives. First, we provide an operational evaluation of the coupled WRF-CMAQ simulation for ozone, particulate matter with diameters less than 2.5 µm ($PM_{2.5}$) and particulate matter with diameters less than 10 µm (PM_{10}) and compare results to the annual application of the uncoupled system performed during AQMEII Phase 1. Next, we evaluate simulated Aerosol Optical Depth (AOD) and AOD/$PM_{2.5}$ relationships. We then present sensitivity simulations that allow us to quantify the impact of direct feedbacks on key meteorological and air quality variables, and to determine whether the modeling design employed in this study may have underestimated these effects. Finally, we compare observed and modeled changes in air quality and radiation between 2006 and 2010, a process referred to as dynamic evaluation by Dennis et al. (2010).

2.Model Setup and Observational Databases

2.1.Model setup

The WRF-CMAQ coupled modeling system was described in Wong et al. (2012). In this application, it was configured using WRFv3.4 and CMAQv5.0.1 (Appel et al., 2013; see also Foley et al., 2010 and Byun and Schere, 2006). Options in WRF include the Morrison microphysics scheme (Morrison et al., 2008), version 2 of the Kain-Fritsch (KF2) cumulus cloud parameterization (Kain, 2004), the Asymmetric Convective Model version 2 (ACM2) for the planetary boundary layer (Pleim, 2007a, b), the Pleim-Xiu land-surface model (Xiu and Pleim, 2001), and the Rapid Radiative Transfer Model for GCMs (RRTMG) (Clough et al., 2005). Options in CMAQ include the CB05-TU chemical mechanism (Whitten et al., 2010; Sarwar et al., 2011a), the AERO6 three mode aerosol module (Appel et al., 2013; also see Simon and Bhave, 2012; Carlton et al., 2010; Foley et al., 2010; Byun and Schere, 2006; and Binkowski and Roselle 2003), wet deposition as described in Byun and Schere (2006) and dry deposition as described in Pleim and Ran (2011).

Biogenic emissions were calculated inline with WRF meteorology using BEIS3.14 (Vukovich at al., 2002; Schwede et al., 2005). Windblown dust emissions were also calculated inline using WRF meteorology (Appel et al., 2013). The direct feedback effects of CMAQ simulated aerosols on RRTMG radiation calculated within WRF were simulated using the approach described in Wong et al. (2012) but updated to use the core-shell method described in Bohren and Huffman (1998). While aerosol indirect effects are included in a research version of WRF-CMAQ (Yu et al., 2014), this version was not available in time for the current application under AQMEII Phase 2; thus, indirect effects are not considered in this study. Photolysis rates were calculated inline in CMAQ and accounted for the radiative effects of simulated aerosols (Binkowski et al., 2007). The modeling system was configured with a 12-km horizontal grid spacing covering the continental U.S. In the vertical, 35 layers were used with a first layer top of approximately 19-m and a top layer pressure of 100 mb. Annual WRF-CMAQ simulations for 2006 and 2010 were performed in a continuous fashion using two or three separate run streams each, with each run stream preceded by a ten day spin up period for model initialization. Throughout the simulations, nudging of temperature, wind speed, and water vapor mixing ratio was applied above the PBL following the approach described in Gilliam et al. (2012). In addition, soil temperature and moisture nudging as described in Pleim and Xiu (2003) and Pleim and Gilliam (2009) was applied as well. However, to avoid squelching the model simulated direct feedback effects, the temperature, wind speed, and water vapor mixing ratio nudging coefficients were reduced by a factor of six compared to Gilliam et al. (2012). The effect of nudging on model performance and the strength of simulated feedback effects is investigated in Section 3.4 using some of the sensitivity simulations listed below.

The preparation of anthropogenic emission inputs for both 2006 and 2010 as well as a comparison against the 2006 emission inventories used in AQMEII Phase 1 is described in Pouliot et al. (2014). Chemical boundary conditions for a number of gas phase species as well as dust, elemental carbon, organic carbon, and sulfate were derived from 3-hrly global fields generated under the Monitoring Atmospheric Composition and Climate (MACC) project (Inness et al., 2013). The MACC fields were horizontally and vertically interpolated to the WRF-CMAQ domain and mapped to the gas phase and aerosol species used in WRF-CMAQ. It should be noted that during the vertical interpolation process, an erroneous assumption was made that the WRF-CMQ model top was at 50 mb rather than 100 mb. As a result of this error which was discovered only after the simulations were completed, upper tropospheric and lower stratospheric ozone simulated by WRF-CMAQ is expected to have a positive bias, a result indeed seen in the analysis of vertical ozone profiles presented in Im et al. (2014) and the evaluation of the tropospheric ozone column against tropospheric ozone residuals from Ozone Monitoring Instrument- Microwave Limb Sounder (OMI-MLS) on Aura (Wang et al., 2014a). However, this error is unlikely to affect any of the results presented in this study.

2.2.Sensitivity Simulations

In addition to the annual 2006 and 2010 WRF-CMAQ simulations described above, several sensitivity simulations were performed to investigate specific aspects of the modeling system. For June – August 2006 and May – September 2010, the coupled WRF-CMAQ system was applied with direct feedback effects turned off to allow a comparison of the feedback and no feedback versions of this modeling system. In this study, the analysis of feedback effects is restricted to June – August since this period was covered in both years. It should be noted that in the no feedback simulation, no default or climatological aerosol profiles were provided to the RRTMG model employed in WRF, thus, there are no aerosol effects on the radiation calculations. To investigate the impact of boundary conditions on changed ozone performance between the AQMEII Phase 1 and AQMEII Phase 2 simulations, January and July 2006 no feedback WRF-CMAQ simulations were performed using chemical boundary conditions derived from global fields from the MACC predecessor project Global and Regional Earth-System Monitoring Using Satellite and In-Situ Data (GEMS) that had been used in AQMEII Phase 1 (Innes et al., 2009; Benedetti et al., 2009; Schere et al., 2012). Finally, to investigate the effects of nudging on model performance and the strength of the simulated feedback effect, sensitivity simulations without nudging were performed for July 2006 for both the direct feedback and no feedback versions of WRF-CMAQ.

2.3.Observations

For model evaluation purposes, observed hourly ozone, $PM_{2.5}$, CO, NO_2, NO_x, NO_y, and SO_2 concentrations as well as observed daily average $PM_{2.5}$ and PM_{10} concentrations were obtained from the

U.S. EPA's Air Quality System (AQS). Depending on the monitor, daily measurements are available every day, every third day, or every sixth day. Daily average observations of $PM_{2.5}$ mass and species were also obtained from the Chemical Speciation Network (CSN) and the Interagency Monitoring of Protected Visual Environments (IMPROVE) network. For some of the analyses, daily maximum 8-hr average ozone (DM8O3) concentrations were estimated from the hourly data. For the evaluation of AOD, we used level 2 data from all AErosol RObotic NETwork (AERONET) sites in the modeling domain. For the evaluation of model predicted clear sky shortwave radiation at the surface, we used the CERES satellite derived Energy Balanced And Filled (EBAF) product edition 2.7 that provides monthly average data (Kato et al., 2013).

3.Results and Discussion

3.1.Operational Model Evaluation And Comparison to AQMEII Phase 1 Results

In this section we provide a comparison of simulated air quality against observations. Table 1a provides seasonal model performance statistics for 2006 for DM8O3 and daily average $PM_{2.5}$ and PM_{10}, while results for 2010 are summarized in Table 1b. Along with the performance metrics for the simulations performed in this study, Table 1a also provides results for the 2006 offline WRF CMAQ4.7.1 simulations performed for AQMEII Phase1 and described in Appel et al. (2012). The results show that except for winter 2010, the online coupled WRF-CMAQ5.0.1 simulations overestimated observed domain mean ozone concentrations for all seasons in both years. While the bias was almost constant throughout the year in 2006, in 2010 it was lower during the winter and higher during the summer. For $PM_{2.5}$, the WRF-CMAQ5.0.1 simulations overestimate concentrations during winter and are almost unbiased during summer for both years. For PM_{10}, concentrations are underestimated in all seasons in 2006 while in 2010, the bias is negative only during spring and fall. For both years and all seasons, correlations are higher for DM8O3 than for $PM_{2.5}$, and correlations for $PM_{2.5}$ are higher than those for PM_{10}.

A comparison of the AQMEII Phase 1 simulations (hereafter referred to as "Phase 1") and those performed in the current study show that the Phase 1 simulations had a lower DM8O3 bias during winter, spring and fall while the summer DM8O3 bias was comparable between both simulations. For $PM_{2.5}$, the positive winter, spring and fall biases present in Phase 1 became more pronounced in the current simulations while during summer time, the current simulations are almost unbiased while the Phase 1 simulations showed a negative bias of 2.4 $\mu g/m^3$. For PM_{10}, the negative biases in the current simulations discussed above are less severe than those in Phase 1. Correlations between model predictions and observations were generally similar between Phase 1 and the current simulations except for $PM_{2.5}$ for which correlations decreased compared to Phase 1.

While it is beyond the scope of the current study to diagnose the reasons behind the differences in model performance for Phase 1 and these simulations, several factors likely played a role. First, relevant model updates in WRF-CMAQ5.0.1 compared to the offline WRF-CMAQ4.7.1 were the inclusion of a wind-blown dust module (Appel et al., 2013), updates to aqueous phase SO_2 oxidation (Sarwar et al., 2011b), and updates to the stable boundary layer treatment (Pleim et al., 2010). These updates tend to increase both $PM_{2.5}$ and PM_{10} concentrations. In addition, the two simulations also utilized different emission estimates and chemical boundary conditions. As discussed in Pouliot et al. (2014), 2006 mobile source NO_x emissions increased by more than 25% from Phase 1 to Phase 2 due to a revised methodology to estimate U.S. mobile source emissions, though emission estimates decreased for several other sectors so that the overall increase in anthropogenic NO_x emissions was roughly 4%. These increased NO_x emissions would be expected to increase region-wide ozone concentrations. Pouliot et al. (2014) also show that methodological updates increased the estimates of primary PM emissions from residential wood combustion and allocated more of these emissions into nighttime hours during which vertical mixing is more limited, likely contributing to the increased positive $PM_{2.5}$ bias in winter and fall.

Besides the updates to the anthropogenic emissions, chemical boundary conditions have also been updated relative to those used in Phase 1 of AQMEII as noted in Section 2.2. To investigate the impacts of the changed lateral boundary conditions on the Phase 2 results, we performed sensitivity simulations for January and July 2006 in which the Phase 2 MACC boundary conditions were replaced by Phase 1 GEMS boundary conditions. Figure 1 shows maps of January and July average ozone differences between these two simulations. In both months, all ozone differences are positive, indicating higher ozone mixing ratios in MACC than GEMS. For January, the differences over large portions of the modeling domain are 7 ppb or greater, while for July, the differences are less than 3 ppb for most of the modeling domain though differences as large as 10 ppb are simulated over the Northwestern U.S. These results suggest that the change in wintertime ozone bias between Phase 1 and Phase 2 simulations depicted in Table 1a is largely driven by the choice of chemical boundary conditions. It is envisioned that the importance of large-scale background concentration simulated by global models on concentrations and source-receptor relationship simulated by regional models will be a key focus of the next Phase of AQMEII.

Overall, the model performance results discussed in this section for the WRF-CMAQ5.0.1 online coupled modeling system are within the range of previous offline regional-scale simulations as summarized in Simon et al. (2012).

3.2.Evaluation of AOD and AOD/$PM_{2.5}$ Relationships

Figures 2a-b show time series of observed and modeled daily AOD at 500 nm for 2006 and 2010, respectively. The time series represent spatial averages over all 29 AERONET sites in the modeling domain that had data coverage in both years. At any given site, model values were only considered for time periods when observations were not missing. These figures reveal a distinct seasonal cycle in both observations and model predictions with a maximum during summer and a minimum during winter. However, model predictions tend to be lower than observations throughout the year, with the underestimation more pronounced during the summer. Such an underprediction is consistent with the evaluation of AOD against observations from the Moderate Resolution Imaging Spectroradiometer (MODIS) satellite presented in Wang et al. (2014a), who reported a normalized mean bias of -34.9%.

One interesting aspect of the results shown in Figure 2 is that the underestimation of AOD occurs throughout all seasons despite the fact that the analysis of 24-hr average surface $PM_{2.5}$ predictions shown in Table 1 revealed overestimations during winter and largely unbiased $PM_{2.5}$ predictions during summer. There are several possible contributors to this phenomenon. First, while the results shown in Table 1 were based on the analysis of filter-based 24-hr average $PM_{2.5}$ measurements and model predictions, no AOD observations and model predictions are available during night time. Thus, any diurnal variation in $PM_{2.5}$ bias would complicate the interpretation of AOD biases in terms of $PM_{2.5}$ biases. Second, while the comparisons shown in Table 1 reflect ground-level concentrations, AOD represents an integration of aerosol extinction over a vertical column. Since model predicted extinctions at any one layer depend not only on aerosol concentrations and properties but also relative humidity, differences in the vertical distribution of modeled aerosol concentrations and relative humidity would yield different calculated AOD even if $PM_{2.5}$ column mass was constant. In other words, overestimated ground level $PM_{2.5}$ concentrations do not necessarily contradict underestimated AOD depending on the vertical distribution of aerosol mass, speciation, number concentration, and relative humidity. Third, the differences between ground-level $PM_{2.5}$ and column total AOD performance might point to the need for further diagnostic testing of the aerosol optics calculations currently implemented in WRF-CMAQ. These calculations are based on the core-shell method described by Bohren and Huffman (1998) (Binkowski and Wong, 2012).

The contribution of the first potential effect is investigated in the following section. It is beyond the scope of this study to further investigate the second and third potential reasons for the apparent disconnect between ground level $PM_{2.5}$ concentration and AOD model performance. However, Curci et al. (2014) provide an analysis of the effects of vertical distribution of $PM_{2.5}$ and relative humidity on calculated AOD. Moreover, Gan et al. (2014) use detailed observations obtained during the Carbonaceous Aerosol and Radiative Effects Study (CARES) field campaign to diagnostically evaluate the WRF-CMAQ aerosol calculations and conclude that the primary reason for discrepancies between observed and simulated optical properties appears to be discrepancies between observed and modeled profiles of aerosol concentrations and composition rather than the optics calculations.

To address whether diurnal variations in $PM_{2.5}$ model performance may play a role in the difference between model performance for 24-hr average $PM_{2.5}$ and hourly AOD, for each of the 29 AERONET sites reporting AOD we determined the closest AQS site reporting hourly $PM_{2.5}$. Next, we considered only those hourly observed and modeled $PM_{2.5}$ concentrations at these sites for which contemporaneous observed and modeled AOD was available at the 29 AERONET sites. Finally, we used these data to compute quarterly average observed and modeled $PM_{2.5}$ concentrations and AOD at each AQS/AERONET station pair for both 2006 and 2010. An analysis of this dataset shows that the resulting $PM_{2.5}$ bias is 1.4, -0.8, -3.9, and 0.3 $\mu g/m^3$ for winter, spring, summer and fall, respectively, when averaged over both 2006 and 2010. Therefore, while winter and fall $PM_{2.5}$ concentrations still tend to be overestimated even when excluding hours with no AOD measurements (predominantly night time), the amount of overestimation is less pronounced than those for the 24-hr average measurements shown in Table 1a-b. Moreover, spring $PM_{2.5}$ concentrations now tend to be slightly underestimated instead of overestimated, and summertime $PM_{2.5}$ concentrations show a substantial underestimation. Figure 3 depicts the observed and simulated relationships between $PM_{2.5}$ and AOD constructed from this dataset. Correlations between observed (modeled) $PM_{2.5}$ and AOD are 0.31 (0.46) for winter, 0.54 (0.47) for spring, 0.50 (0.56) for summer, and 0.58 (0.46) for fall, showing that the model simulations capture the strengthening of the observed $PM_{2.5}$/AOD relationship during spring and summer. Linear regressions through the origin show observed (simulated) AOD vs. $PM_{2.5}$ slopes of 0.008 (0.004) for winter, 0.012 (0.009) for spring, 0.012 (0.011) for summer, and 0.009 (0.006) for fall. These slopes, along with a visual comparison of the observed and modeled AOD vs. $PM_{2.5}$ scatter plots in Figure 3 suggest that, despite the change in $PM_{2.5}$ model performance when considering hourly observations during daytime rather than 24-hr average concentrations, the observed relationship between AOD and $PM_{2.5}$ is not fully captured by the model. Future research, as discussed in the previous paragraph, is needed to further investigate these discrepancies.

3.3. Strength of Simulated Direct Feedback Effects

In this section, we quantify the aerosol direct radiative effects on several simulated meteorological and air quality fields by contrasting these fields against those from a simulation that did not consider aerosol direct feedback effects. The twelve panels in Figure 4 show maps of June – August average AOD as well as differences in June – August average clear-sky shortwave radiation at the ground, temperature, planetary boundary layer (PBL) height, ozone, and $PM_{2.5}$ between the feedback and no feedback simulations, for both 2006 and 2010. All fields were calculated over all daytime hours. The AOD maps show higher values over the eastern U.S. compared to the western U.S., consistent with higher aerosol concentrations in these regions. As expected, the differences in clear-sky shortwave radiation at the ground between the feedback and no feedback simulations are consistently negative, reflecting the extinction by aerosols in the feedback simulations that was not considered in the no-feedback simulations. The spatial pattern of the differences in clear-sky shortwave radiation aligns closely with the patterns in AOD, with areas of higher AOD corresponding to areas with higher reduction in radiation. Reductions in daytime summer average clear-sky shortwave radiation range from about 5 W/m^2 in the western U.S. to about 20 W/m^2 in the eastern U.S. These reductions in radiation cause decreases in 2-m temperature and PBL heights, with the spatial patterns of the temperature showing more similarities with those of the AOD and radiation compared to those of PBL heights. The largest simulated daytime average temperature decreases are on the order of 0.1 K, while the typical reductions in PBL height range from 10m to 30m. The effects on daytime average ozone mixing ratios vary in space: ozone concentrations tend to increase in the central and southern portion of the modeling domain while they decrease over the northeastern and western portion as well as Canada. Negative differences are also simulated for many urban areas, indicating that decreased ventilation may lead to increased titration. The majority of the ozone differences is less than +/- 0.25 ppb. For $PM_{2.5}$, 2006 concentrations increase by up to 0.6 $\mu g/m^3$ over the eastern U.S. due to feedback effects, though most of the increases are on the order of 0.2 $\mu g/m^3$. For 2006, both positive and negative changes can be seen over parts of the northwest, an area of active wildfires during the analysis period. The effect of wildfires on simulated feedbacks is discussed in Makar et al. (2014a, b).

In general, it can also be seen that the feedback effects were stronger in 2006 and 2010, consistent with the higher AOD estimated for the earlier year. The change of the strength of the feedback effect over time will be further discussed in Section 3.5. It also should be noted that the analysis in this section focused on average changes over a three-month period. Makar et al. (2014a, b) present a multi-model comparison of feedback vs. no feedback simulations and highlight case studies during which feedback effects are stronger. Moreover, using two different online-coupled models, Makar et al. (2014a, b) and Wang et al. (2014b) also show that aerosol indirect effects (not included in this WRF-CMAQ simulation) tend to have a stronger impact on both meteorological and air quality variables than aerosol direct effects. Finally, it should be mentioned that the effects of the direct feedback effects shown here are smaller than other factors affecting model performance such as emissions or the changes in chemical boundary conditions discussed in Section 3.1.

3.4. Effect of Nudging on Model Performance and Simulated Direct Feedback Effect

As stated in Section 2.1, the WRF-CMAQ simulations analyzed in this study applied nudging to temperature, winds, and water vapor mixing ratio above the PBL as well as soil temperature and moisture throughout the simulation. While such nudging has been shown to improve the characterization of meteorological conditions for retrospective air quality simulations (Otte, 2008; Gilliam and Pleim, 2010; Gilliam et al., 2012), these studies were performed with offline modeling system in which there was no feedback from the air quality to the meteorology. When designing the AQMEII Phase 2 modeling protocols, most modeling groups felt that no nudging should be applied to coupled modeling systems since the forcing exerted by the nudging term may be stronger than the feedback effects to be studied. Thus, by including nudging in our WRF-CMAQ simulations, our setup differs from that of all other AQMEII Phase 2 simulations which used overlapping 72-hr simulation periods consisting of a 24-hr spin-up period after meteorological initialization during which nudging can be used followed by a 48-hr "forecast" period that was then used for subsequent analyses. To assess the impact of nudging on both model performance and the strength of the simulated direct feedback effect, we performed sensitivity simulations for July 2006 in which WRF-CMAQ was applied both with and without direct feedback effects following the 72-hr block modeling approach used by other groups.

Figure 5a shows a time series of 2-m temperature bias for the direct feedback and no feedback simulations utilizing nudging as discussed above as well as the sensitivity simulations using no nudging. The time series reflect averages over all sites in the modeling domain from June 30 – July 31, 2006 and are depicted as a function of hours since the beginning of each 48-hr forecast period. In other words, "hour 0" represents the average over 00:00 GMT on June 30, July 2, … July 30, "hour 1" represents the average over 01:00 GMT on June 30, July 2, … July 30, and so on. The results show that the model biases for the no nudging simulations are always positive while the biases for the nudging simulations oscillate around zero. The positive biases for all simulations peak during the early morning hours (hour 0 represents 00:00 GMT and the analysis is conducted over North America). The biases are larger for the no-nudging simulations than for the nudging simulations and also increase over time (0.8 C on day 1 and 0.9 C on day 2), reflecting a gradual departure from the observed state of the atmosphere. Thus, nudging does appear to have the intended effect on simulated temperature fields. This is also confirmed by a comparison of 2-m temperature performance from the 2010 annual WRF-CMAQ simulations using nudging against the performance of the other AQMEII Phase 2 simulations over North America that did not use nudging. As shown in Brunner et al. (2014), WRF-CMAQ temperature errors typically are lower than those from other modeling systems.

While Figure 5a establishes that nudging had the intended effect on temperature performance during July 2006, it is difficult to discern to what extent nudging may have dampened the strength of the simulated feedback effect, since the difference in model bias between the nudging and no nudging simulations is larger than the differences between the feedback and no feedback simulations for either set of simulations. To better illustrate the effect, Figure 5b shows time series of the difference between the feedback and no feedback cases for both the nudging and no nudging model configurations. These results illustrate that the changes in the simulated direct feedback effects due to employing a nudging approach are generally small compared to the no nudging approach employed by other AQMEII Phase 2 groups. Thus, these sensitivity simulations suggest that even in feedback simulations, weak nudging can be beneficial in improving the representation of atmospheric conditions relevant to retrospective air quality applications without overwhelming the strength of the simulated feedback effects. However, future research is needed to determine the optimal balance between these two competing objectives for a wider range of atmospheric conditions than the single month considered in this sensitivity analysis.

3.5. Dynamic Evaluation: 2006 – 2010

In this section, we focus on the ability of the coupled modeling system to simulate observed changes in air quality and radiation between 2006 and 2010. As shown in Table 3 of Pouliot et al. (2014), the 2006 and 2010 emissions inventories developed for AQMEII Phase 2 show decreases in annual total anthropogenic SO_2, NO_x, non-methane volatile organic compounds (NMVOC), and $PM_{2.5}$ emissions over the U.S. of 29%, 17%, 4% and 12%, respectively, due to the implementation of control programs as well as vehicle fleet turnover. While most of the SO_2 reductions occurred year-round, NO_x reductions in most states were mainly effective during wintertime because a number of states had already reduced summertime NO_x emissions from power plants in 2004 due to an earlier control program. In addition to these changes in emissions, the year-to-year changes in meteorology shown in Stoeckenius et al. (2014) are also expected to influence observed and simulated air quality concentrations.

Figures 6a-h show bar charts of absolute and relative changes in quarterly gas-phase concentrations (averaged across all sites) for both observations and model predictions, while Figures 7a-h show corresponding results for $PM_{2.5}$ concentrations. The results for summertime DM8O3 show that the model underestimates the observed decreases, similar to earlier results for other years (Gilliland et al., 2008). Absolute changes in summertime daily average NO_x are overestimated, but relative changes are captured, pointing to a systematic overestimation of absolute concentrations. Changes in summertime daily average SO_2 concentrations are similar between observations and model simulations both in an absolute and relative sense. During winter and spring, the model predicted decreases for both DM8O3 and hourly ozone while there was little change or even a small increase in the observations. The discrepancy likely arises from a combination of ozone lateral boundary conditions and the inability to adequately represent ozone titration at urban monitors with the 12km grid resolution used here. During fall, neither observations nor WRF-CMAQ showed appreciable changes for these two variables. The results for total and speciated $PM_{2.5}$ vary between quarters, networks and species. During summer, absolute and relative modeled changes frequently are close to observed changes. The comparison to other quarters also shows that the $PM_{2.5}$ changes are largest in summer and fall for both observations and model simulations. Separate analysis (not shown here) indicates that the spatial patterns of observed and modeled changes generally align, indicating that the spatial patterns of emission changes as well as the modifying effects of interannual meteorological variability are generally captured. For example, both observations and model predictions show only small changes in summertime DM8O3 in the Northeastern U.S. while larger decreases are seen for the west coast and the southern portion of the modeling domain. This is consistent with both the differences in meteorology (2010 temperatures were warmer in the Northeast and cooler in the West) and summertime NO_x emission reductions (power plants emission reductions were larger in the South than the Northeast).The directionality of the change im summertime DM8HO3 was captured at 90% of all sites.

Figure 8a shows a map of 2010 – 2006 differences in simulated June - August average $PM_{2.5}$ concentrations. Decreases of 2-3 $\mu g/m^3$ are visible over large portion of the Eastern U.S. as well as over the Northwestern U.S. Figure 8b shows that the areas of the largest $PM_{2.5}$ decreases experienced an increase in average clear-sky shortwave radiation between 5 and 10 W/m^2. These changes in simulated clear-sky shortwave radiation can be compared to corresponding data from the CERES satellite products, shown in Figure 8c. This comparison shows that the WRF-CMAQ system captured the broad spatial changes in shortwave radiation between 2006 and 2010 but underestimated the magnitude of the CERES-derived change. Part of this underestimation may be caused by the tendency of WRF-CMAQ to underestimate AOD as shown in Section 3.2.

While the results shown above illustrated the coupled modeling system's ability to respond to changed forcings from emissions, meteorology, and background concentrations, it is also of interest to determine how different the simulated change would be if a traditional offline modeling system had been applied. To this end, we calculated the changes in June – August daytime average $PM_{2.5}$ concentrations between 2006 and 2010 using both the base model configuration including direct feedback effects and the sensitivity simulations discussed in Section 3.3 that did not include feedback effects. Figures 9a-b show the differences in the simulated change between the feedback and no feedback simulations, both in an absolute sense as well as normalized by the change simulated in the no-feedback configuration. These figures illustrate that the decrease in daytime average $PM_{2.5}$ simulated by the feedback case is 0.2 – 0.4 $\mu g/m^3$ larger over portions of the eastern U.S. than the decrease simulated by the no feedback case. In other words, the direct feedback effects in the coupled modeling system cause an "emission control dividend" associated with reducing SO_2 emissions (reduced SO_2 emissions reduce sulfate concentrations which in turn increase solar radiation and PBL height which then causes a further reduction in $PM_{2.5}$ concentrations due to enhanced ventilation), and this dividend is on the order of 5-10% of the change simulated by the no feedback modeling system.

4.Summary

In this study, we presented an application of the online coupled WRF-CMAQ modeling system (Wong et al., 2012) to two annual simulations over North America performed under AQMEII Phase 2. Through operational model evaluation, it was shown that model performance of the coupled modeling system is comparable to earlier annual applications of the uncoupled WRF/CMAQ modeling system such as the 2006 simulations performed under AQMEII Phase 1. A comparison of the AOD simulated by the coupled modeling system against observations from AERONET revealed a tendency toward underprediction in all seasons despite a tendency to overpredict $PM_{2.5}$ during wintertime. Future research is needed to further investigate the reasons behind this model behavior, such as potential differences in observed and modeled vertical profiles of speciated $PM_{2.5}$ mass and size distributions as well as relative humidity.

By comparing results from the coupled WRF-CMAQ simulation against sensitivity simulations without direct effects performed for June – August 2006 and 2010, it was possible to determine the average impact of the simulated direct feedback effect on temperature, PBL heights, ozone and $PM_{2.5}$ concentrations. The largest simulated seasonal mean daytime average temperature decreases were found to be on the order of 0.1 K while the typical reductions in PBL height ranged from 10-m to 30-m. The effects on daytime average ozone concentrations varied in space and the majority of the ozone differences were less than +/- 0.25 ppb. For $PM_{2.5}$, 2006 concentrations increased by up to 0.6 $\mu g/m^3$ over the eastern U.S. due to direct feedback effects, though most of the increases were on the order of 0.2 $\mu g/m^3$.

As opposed to other modeling groups participating in AQMEII Phase 2, the WRF-CMQ simulations analyzed in this study used nudging of select meteorological variables to improve the characterization of the meteorological fields relevant to air quality. It was shown through a one-month sensitivity simulation that the nudging approach improved performance for 2-m temperature while it had only a small dampening effect on the strength of the simulated direct feedbacks. Future research is needed to develop a nudging approach that optimizes the trade-off between improved model performance and allowing the model to respond to forcings from feedback effects.

Model results for 2006 and 2010 were also analyzed to compare modeled changes between these years to those seen in observations. The WRF-CMAQ simulations captured the substantial decreases in observed $PM_{2.5}$ concentrations in summer and fall. For summertime $PM_{2.5}$, decreases of 2-3 $\mu g/m^3$ were visible over a large portion of the Eastern U.S. as well as over the Northwestern U.S. In the WRF-CMAQ simulations, these areas saw a resulting increase in daytime average clear-sky shortwave radiation between 5 and 10 W/m^2. When these changes in simulated clear-sky shortwave radiation were compared to corresponding data from the CERES satellite, results showed that the WRF-CMAQ system captured the broad spatial changes in shortwave radiation between 2006 and 2010 but underestimated the magnitude of the CERES-derived change. Furthermore, analysis of sensitivity simulations performed with the no-feedback version of WRF-CMAQ showed that the 2006-2010 decrease in daytime average $PM_{2.5}$ simulated by the feedback configuration is 0.2 – 0.4 $\mu g/m^3$ larger over portions of the eastern U.S. than the decrease simulated by the no feedback configuration. In other words, the feedback simulations suggest that there is an "emission control dividend" from reducing $PM_{2.5}$ precursor emissions such as SO_2 that is not captured in traditional no feedback model applications, and this dividend is on the order of 5-10% of the change simulated by the no feedback modeling system. Future work is needed to quantify this dividend over longer time periods and regions with different emission trends.

In summary, this application of the coupled WRF-CMAQ modeling system as part of AQMEII Phase 2 presents a first step in using this system to study aerosol/radiation interactions under changing emissions and meteorological forcings. Future work will focus on applying and evaluating this system over longer time periods, different regions, and different spatial scales (Xing et al., 2014). Work will also be performed to apply and evaluate a model version incorporating indirect effects (Yu et al., 2014) to more fully account for interactions between aerosols, radiations and clouds. In closing, it should be noted that while the coupled WRF-CMAQ system allows the analysis of phenomena that could not be studied with the traditional no feedback approach, many factors known to affect offline regional scale model performance (emissions, boundary conditions) still tend to be more important to overall model performance compared to transitioning from a no feedback to a feedback modeling approach.

Acknowledgments and Disclaimer

The views expressed here are those of the authors and do not necessarily reflect the views and policies of the U.S. Environmental Protection Agency (EPA) or any other organization participating in the AQMEII project. This paper has been subjected to EPA review and approved for publication. We gratefully acknowledge the contribution of various groups for the datasets used in this study. Chemical boundary conditions were obtained from the ECMWF/MACC project and Météo-France/CNRM-GAME. The CERES data used in this analysis were obtained from the NASA Langley Research Center Atmospheric Science Data Center. We thank the principal investigators and their staff for establishing and maintaining the AERONET sites used in this study.

References

Appel, K. W., G.A. Pouliot, H. Simon, G. Sarwar, H.O.T. Pye, S.L. Napelenok, F. Akhtar, and S.J. Roselle, 2013. Evaluation of dust and trace metal estimates from the Community Multiscale Air Quality (CMAQ) model version 5.0, Geosci. Model Dev., 6, 883-899, doi:10.5194/gmd-6-883-2013

Baklanov, A., et al., 2014. Online coupled regional meteorology chemistry models in Europe: current status and prospects. Atm. Chem. Phys. 14, 317-398.

Benedetti, A., J.-J. Morcrette, O. Boucher et al., 2009: Aerosol analysis and forecast in the European Centre for Medium-Range Weather Forecasts Integrated Forecast System: 2. Data assimilation, J. Geophys. Res., 114 (D13205), doi:10.1029/2008JD011115

Binkowski, F. S., and S. J. Roselle, 2003, Models-3 Community Multiscale Air Quality (CMAQ) model aerosol component, 1, Model description, J. Geophys. Res., 108, 4183, doi:10.1029/2001JD001409

Binkowski, F.S., S. Arunachalam, Z. Adelman, and J.P. Pinto, 2007: Examining Photolysis Rates with a Prototype Online Photolysis Module in CMAQ. J. Appl. Meteor. Climatol., 46, 1252–1256.

Binkowski, F.S., and D. Wong, 2012: Correctly representing the optical properties of black carbon in the integrated WRF-CMAQ system, Presentation at the 11th Annual CMAS Models-3 User's Conference, October 2012, Chapel Hill, NC, available online at http://cmascenter.org/conference/2012/slides/binkowski_correctly_representing_2012.ppt

Bohren, C.F. and D.R. Huffman, Absorption and scattering of light by small particles, New York: Wiley, 1998, 530 p., ISBN 0-471-29340-7, ISBN 978-0-471-29340-8 (second edition)

Byun, D. W. and K.L. Schere, 2006. Review of the governing equations, computational algorithms, and other components of the Models- 3 Community Multiscale Air Quality (CMAQ) Modeling System, Appl. Mech. Rev., 59, 51–77

Carlton, A. G., P. Bhave, S. Napelenok, E. O. Edney, G. Sarwar, R. W. Pinder, G. Pouliot, and M. Houyoux, 2010. Model Representation of Secondary Organic Aerosol in CMAQ v4.7. Environmental Science & Technology, 44, 8553-8560

Clough, S. A., M.W. Shephard, E.J. Mlawer, J.S. Delamere, M.J. Iacono, K. Cady-Pereira, S. Boukabara, and P.D. Brown, 2005. Atmospheric radiative transfer modeling: a summary of the AER codes, J. Quant. Spectrosc. Ra., 91, 233–244

Curci, G., et al., 2014, Uncertainties of simulated aerosol optical properties induced by assumptions on aerosol physical and chemical properties: An AQMEII-2 perspective, Atmos. Environ., in press, doi:10.1016/j.atmosenv.2014.09.009

Foley, K. M., et al., 2010, Incremental testing of the Community Multiscale Air Quality (CMAQ) modeling system version 4.7, Geosci. Model Dev., 3, 205–226, doi:10.5194/gmd-3-205-2010

Gan, C.M., F. Binkowski, J. Pleim, J. Xing, D. Wong, R. Mathur, and R. Gilliam, 2014, Assessment of the aerosol optics component of the coupled WRF–CMAQ model using CARES field campaign data and a single column model, Atmos. Environ, in press, doi:10.1016/j.atmosenv.2014.11.028

Gilliam, R.C., and J.E. Pleim, 2010. Performance assessment of new land surface and planetary boundary layer physics in the WRF-ARW. J. Appl. Meteor. Climatol. 49, 760-774

Gilliam, R.C., J. M. Godowitch, and S. T. Rao, Improving the horizontal transport in the lower troposphere with four dimensional data assimilation, Atmos. Environ., 53, 186-201, doi:10.1016/j.atmosenv.2011.10.064

Gilliland, A.B., C. Hogrefe, R. W. Pinder, J. M. Godowitch, K. L. Foley, and S.T. Rao, 2008: Dynamic evaluation of regional air quality models: Assessing changes in O_3 stemming from changes in emissions and meteorology, Atmos. Environ., 42, 5110-5123, doi:10.1016/j.atmosenv.2008.02.018

Grell, G.A., S.E. Peckham, R. Schmitz, S.A. McKeen, G. Frost, W.C. Skamarock, B. Eder, 2005. Fully coupled online chemistry within the WRF model. Atmos. Environ. 39, 6957-6975.

Im, U., et al., 2014, Evaluation of operational on-line-coupled regional air quality models over Europe and North America in the context of AQMEII phase 2. Part I: Ozone, Atmos. Environ., in press, doi:10.1016/j.atmosenv.2014.09.042

Inness, A., J. Flemming, M. Suttie, L. Jones, 2009: GEMS Data Assimilation System for Chemically Reactive Gases, Technical Memorandum No. 587 European Centre for Medium-Range Weather Forecasts (ECMWF), UK, Reading

Inness, A., et al, 2013: The MACC reanalysis: an 8 yr dataset of atmospheric composition, Atmos. Chem. Phys., 13, 4073-4109, doi:10.5194/acp-13-4073-2013

Kain, J. S., 2004. The Kain-Fritsch convective parameterization: an update, J. Appl. Meteorol., 43, 170–181

Kato, S., N. G. Loeb, F. G. Rose, D. R. Doelling, D. A. Rutan, T. E. Caldwell, L. Yu, R. A. Weller, 2013: Surface Irradiances Consistent with CERES-Derived Top-of-Atmosphere Shortwave and Longwave Irradiances. J. Climate, 26, 2719–2740, doi:10.1175/JCLI-D-12-00436.1

Makar, P.A., et al., 2014a, Feedbacks between Air Pollution and Weather, Part 1: Effects on Weather, Atmos. Environ., in press, doi:10.1016/j.atmosenv.2014.12.003

Makar, P.A., et al. 2014b, Feedbacks between air pollution and weather, part 2: Effects on chemistry, Atmos. Environ., in press, doi: 10.1016/j.atmosenv.2014.10.021

Morrison, H., G. Thompson, V. Tatarskii, 2009. Impact of Cloud Microphysics on the Development of Trailing Stratiform Precipitation in a Simulated Squall Line: Comparison of One- and Two-Moment Schemes. Mon. Wea. Rev., 137, 991–1007. doi:10.1175/2008MWR2556.1

Otte, T.L., 2008. The impact of nudging in the meteorological model for retrospective air quality simulations. part I: evaluation against national observation networks. J. Appl. Meteor. Climatol. 47, 1853-1867.

Pleim, J. E., 2007a. A combined local and nonlocal closure model for the atmospheric boundary layer. Part I: model description and testing, J. Appl. Meteorol. Clim., 46, 1383–1395

Pleim, J. E., 2007b. A combined local and nonlocal closure model for the atmospheric boundary layer. Part II: application and evaluation in a mesoscale meteorological model, J. Appl. Meteorol. Clim., 46, 1396–1409

Pleim, J. E. and R. Gilliam, 2009. An indirect data assimilation scheme for deep soil temperature in the Pleim-Xiu land surface model, J. Appl. Meteorol. Clim., 48, 1362–1376

Pleim, J. and L. Ran, 2011. Surface Flux Modeling for Air Quality Applications. Atmosphere, 2, 271-302

Pleim, J., R. Gilliam, and J. Godowitch, 2010: Evaluation of PBL models compared to GABLS experiments and testing in meteorology and air quality models, presented at the 19th Symposium on Boundary Layers and Turbulence, American Meteorological Society, August 2–6, 2010, Keystone, CO, recorded presentation available at http://ams.confex.com/ams/19Ag19BLT9Urban/recordingredirect.cgi/id/15728

Pleim, J. E. and A. Xiu, 2003. Development of a land surface model. Part II: data assimilation, J. Appl. Meteorol., 42, 1811–1822

Pouliot, G., H. D. van der Gon, J. Kuenen, J. Zhang, M.D. Moran, and P. Makar, 2014, Analysis of the emission inventories and model-ready emission datasets of Europe and North America for phase 2 of the AQMEII project, Atmos. Environ., in press, doi: 10.1016/j.atmosenv.2014.10.061

Sarwar, G., K.W. Appel, A.G. Carlton, R. Mathur, K. Schere, R. Zhang, and M.A. Majeed, 2011a: Impact of a new condensed toluene mechanism on air quality model predictions in the US, Geosci. Model Dev., 4, 183-193, doi:10.5194/gmd-4-183-2011

Sarwar, G., K. Fahey, S. Napelenok, S. Roselle, R. Mathur, 2011b. Examining the impact of CMAQ model updates on aerosol sulfate predictions, Presentation at the 10th Annual CMAS Models-3 User's Conference, October 2011, Chapel Hill, NC, available online at http://www.cmascenter.org/conference/2011/slides/sarwar_examining_impact_2011.pdf

Schere, K., et al., 2012. Trace gas/aerosol boundary concentrations and their impacts on continental-scale AQMEII modeling domains, Atmos. Environ., 53, 38-50, doi:10.1016/j.atmosenv.2011.09.043

Schwede, D., G.A. Pouliot, and T. Pierce, 2005. Changes to the Biogenic Emissions Inventory System Version 3 (BEIS3), In Proceedings of the 4th CMAS Models-3 Users' Conference, Chapel Hill, NC, 26–28 September 2005

Simon, H., and P.V. Bhave, 2012. Simulating the degree of oxidation in atmospheric organic particles. Environ. Sci. Technol. 46, 331-339

Simon, H., K. R. Baker, and S. Phillips, 2012: Compilation and interpretation of photochemical model performance statistics published between 2006 and 2012, Atmos. Environ., 61, 124-139, doi:10.1016/j.atmosenv.2012.07.012

Skamarock, W. C. et al., 2008. A description of the Advanced Research WRF version 3, National Center for Atmospheric Research Tech. Note, NCAR/TN- 475+STR, 113 pp.

Stoeckenius, T., C. Hogrefe, C. Chemel, J. Zagunisa, T. Sturtza, and T. Sakulyanontvittaya, 2014. A Comparison between 2010 and 2006 Air Quality and Meteorological Conditions, and Emissions and Boundary Conditions used in Simulations of the AQMEII-2 North American Domain, Atmos. Environ., under review

Vukovich, J. and T. Pierce, 2002. The Implementation of BEIS3 within the SMOKE Modeling Framework, in: Proceedings of the 11th International Emissions Inventory Conference, Atlanta, Georgia, available at: www.epa.gov/ttn/chief/conference/ei11/modeling/vukovich.pdf, 15–18 April 2002

Wang, K., et al., 2014a, A multi-model assessment for the 2006 and 2010 simulations under the Air Quality Model Evaluation International Initiative (AQMEII) Phase 2 over North America: Part II. Evaluation of column variable predictions using satellite data, Atmos. Environ., in press, doi: 10.1016/j.atmosenv.2014.07.044

Wang, K., Y. Zhang, K. Yahya, S.-Y. Wu, G. Grell, 2014b, Implementation and Initial Application of New Chemistry-Aerosol Options in WRF/Chem for Simulating Secondary Organic Aerosols and Aerosol Indirect Effects for Regional Air Quality, Atmos. Environ., in press, doi: 10.1016/j.atmosenv.2014.12.007

Whitten, G. Z., G. Heo, Y. Kimura, E. McDonald-Buller, D. Allen, W.P.L. Carter, and G. Yarwood, 2010. A new condensed toluene mechanism for Carbon Bond: CB05-TU, Atmos. Environ., 44, 5346–5355

Wong, D. C., et al., 2012. WRF-CMAQ two-way coupled system with aerosol feedback: software development and preliminary results, Geosci. Model Dev., 5, 299-312, doi:10.5194/gmd-5-299-2012

Xing, J., et al., 2014. Observations and modeling of air quality trends over 1990–2010 across the Northern Hemisphere: China, the United States and Europe, Atmos. Chem. Phys. Discuss., 14, 25453-25501, doi:10.5194/acpd-14-25453-2014

Xiu, A. and J.E. Pleim, 2001. Development of a land surface model. Part I: application in a mesoscale meteorological model, J. Appl. Meteorol., 40, 192–209

Yu, S., R. Mathur, J. Pleim, D. Wong, R. Gilliam, K. Alapaty, C. Zhao, and X. Liu, 2014: Aerosol indirect effect on the grid-scale clouds in the two-way coupled WRF-CMAQ: model description, development, evaluation and regional analysis, Atmos. Chem. Phys., 14, 11247-11285, doi:10.5194/acp-14-11247-2014

Zhang, Y., 2008, Online Coupled Meteorology and Chemistry models: History, Current Status, and Outlook, Atmos. Chem. Phys., 8, 2895-2932.

List of Tables and Figures

Figure 6: Observed and simulated differences in quarterly average concentrations of several gas phase species observed at AQS monitors between 2010 and 2006. Absolute changes are shown on the left while relative changes are shown on the right. Absolute changes for CO have been divided by 100 to be accommodated on the same vertical scale.

Figure 7: As in Figure 6 but for $PM_{2.5}$ total mass, select $PM_{2.5}$ species, and PM_{10} total mass. Absolute changes for PM_{10} have been divided by 10 to be accommodated on the same vertical scale. Letters in parenthesis indicate the monitoring network: A – AQS, I – IMPROVE, C - CSN.

Figure 8: a) Differences in model simulated $PM_{2.5}$ concentrations between 2010 and 2006 averaged over all June – August daytime hours. b) as in a) but for clear-sky shortwave radiation at the surface. c) as in b) but for CERES satellite observations rather than WRF-CMAQ model simulations.

Figure 9: a) Differences in 2010-2006 changes of June – August daytime average $PM_{2.5}$ concentrations between the feedback and no feedback configurations of the WRF-CMAQ modeling system. Cool colors indicate areas where the feedback configuration simulated greater reductions (or smaller increases) between 2010 and 2006 than the no feedback configuration, while the opposite holds true for the areas indicated in warm colors. b) as in a) but normalized by the 2010-2006 change simulated by the no feedback configuration and converted to a percentage scale.

Table 1a. Model performance statistics for the 2006 WRF-CMAQ AQMEII Phase 2 simulations of daily maximum 8-hr ozone, daily average $PM_{2.5}$ and daily average PM_{10} across all AQS sites in the modeling domain. Results for the AQMEII Phase 1 simulations described in Appel et al. (2012) are shown for comparison. MB stands for Mean Bias, ME stand for Mean Error, RMSE stands for Root Mean Square Error, NMB stands for Normalized Mean Bias, NME stands for Normalize Mean Error, and R stands for the correlation coefficient.

Pollutant	Season	Mean Observed (ppb or µg/m^3)	AQMEII Study	MB (ppb or µg/m^3)	ME (ppb or µg/m^3)	RMSE (ppb or µg/m^3)	NMB (%)	NME (%)	R
Daily Maximum 8-hr O_3	Winter	32.3	Phase 2	6.6	8.6	10.6	20.5	26.6	0.71
			Phase 1	0.1	5.6	7.4	0.4	17.2	0.72
	Spring	47.7	Phase 2	6.3	8.9	11.2	13.2	18.7	0.69
			Phase 1	-0.9	6.6	8.6	-1.9	13.8	0.72
	Summer	51.1	Phase 2	5.8	10.4	13.8	11.3	20.4	0.71
			Phase 1	6.5	10.9	14.4	12.7	21.3	0.7
	Fall	39.5	Phase 2	5.9	9	11.2	15	22.8	0.75
			Phase 1	2.2	6.9	9.3	5.6	17.4	0.78
$PM_{2.5}$	Winter	11.4	Phase 2	6.8	9.3	15.7	59.8	81.4	0.51
			Phase 1	3.4	6.1	10.7	30	54	0.51
	Spring	10.7	Phase 2	2.8	5.8	9.1	26.3	54.5	0.45
			Phase 1	0.6	4.2	6	5.2	39.4	0.63
	Summer	14.3	Phase 2	0.2	5.8	8.7	1.4	40.7	0.51
			Phase 1	-2.4	4.9	6.6	-16.7	34.1	0.69
	Fall	11	Phase 2	6.1	7.9	13.2	55.3	72.1	0.55
			Phase 1	3.4	5.5	8.8	31.2	49.8	0.65
PM_{10}	Winter	31.6	Phase 2	-8.7	24.5	139.7	-27.4	77.6	0.01
			Phase 1	-21	23.6	127.4	-66.2	74.4	-0.02
	Spring	25.7	Phase 2	-5.6	20.1	44.2	-22	78.3	0.03
			Phase 1	-18.2	19.4	44.1	-68.8	73.5	0.01
	Summer	30	Phase 2	-6	22.2	43.1	-20	74	0.07
			Phase 1	-22	22.6	41.7	-71.5	73.5	0.06
	Fall	28.4	Phase 2	-1.3	23.6	53.4	-4.4	83.3	0.05
			Phase 1	-18.3	20.3	48.4	-63.2	70.3	0.03

Table 1b: As in Table 1a but for 2010. No AQMEII Phase 1 results are available for this year.

Pollutant	Season	Mean Observed (ppb or $\mu g/m^3$)	AQMEII Study	MB (ppb or $\mu g/m^3$)	ME (ppb or $\mu g/m^3$)	RMSE (ppb or $\mu g/m^3$)	NMB (%)	NME (%)	R
Daily Maximum 8-hr O_3	Winter	33.6	Phase 2	-1.9	6.8	8.8	-5.6	20.2	0.58
	Spring	47.5	Phase 2	2.3	6.6	8.7	4.8	13.9	0.68
	Summer	44.4	Phase 2	6.6	9.7	12.2	14.9	21.8	0.75
	Fall	41.1	Phase 2	3.2	6.9	9.1	7.8	16.7	0.78
$PM_{2.5}$	Winter	11.4	Phase 2	6.5	8.8	14	56.6	76.9	0.53
	Spring	9.2	Phase 2	3.7	5.8	9.3	39.7	63.6	0.54
	Summer	11.1	Phase 2	-0.1	4.5	6.6	-1.1	40.3	0.51
	Fall	9.1	Phase 2	5	6.3	10.1	55.1	69.5	0.59
PM_{10}	Winter	20.7	Phase 2	1.5	16.2	34.6	7.4	78	0.11
	Spring	24.7	Phase 2	-3.6	20.9	69.5	-14.8	84.8	0.04
	Summer	23.9	Phase 2	-1.8	19.7	37	-7.5	82.6	0.07
	Fall	22.7	Phase 2	2.2	19.9	39.6	9.6	87.5	0.12

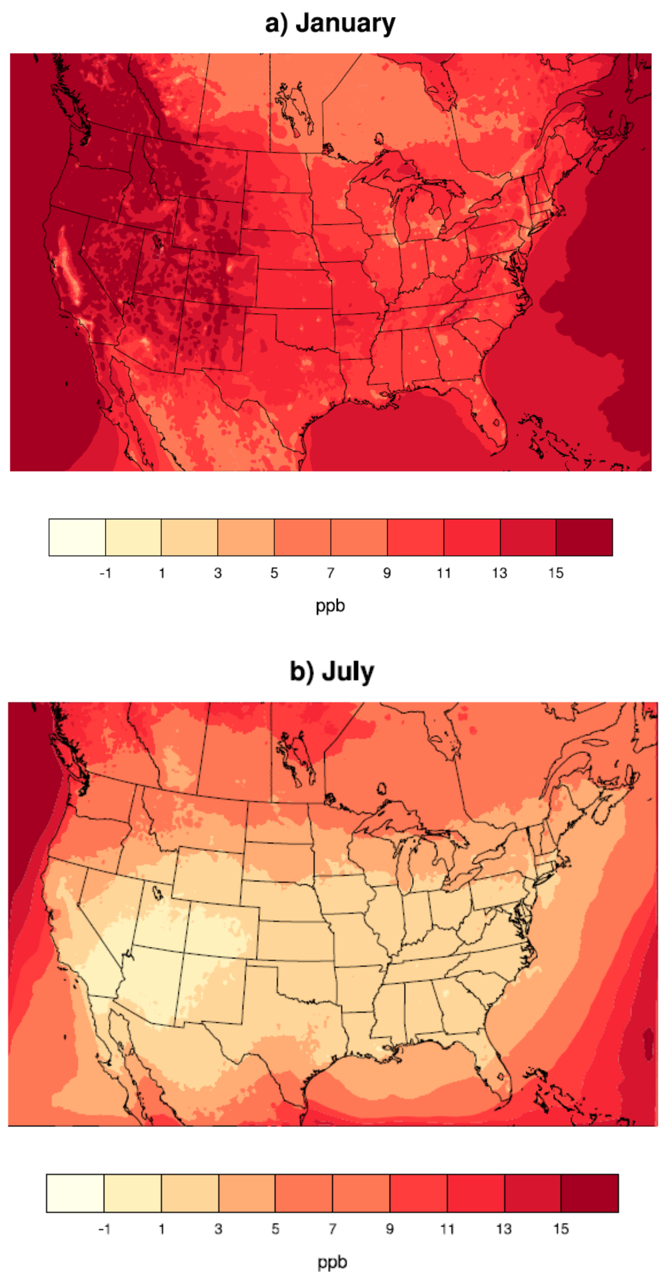

Figure 1: Differences in WRF-CMAQ simulated monthly mean ozone mixing ratios between the base simulation using the MACC boundary conditions provided for AQMEII Phase 2 and the sensitivity simulations using the GEMS boundary conditions provided for AQMEII Phase1. a) January 2006 and b) July 2006.

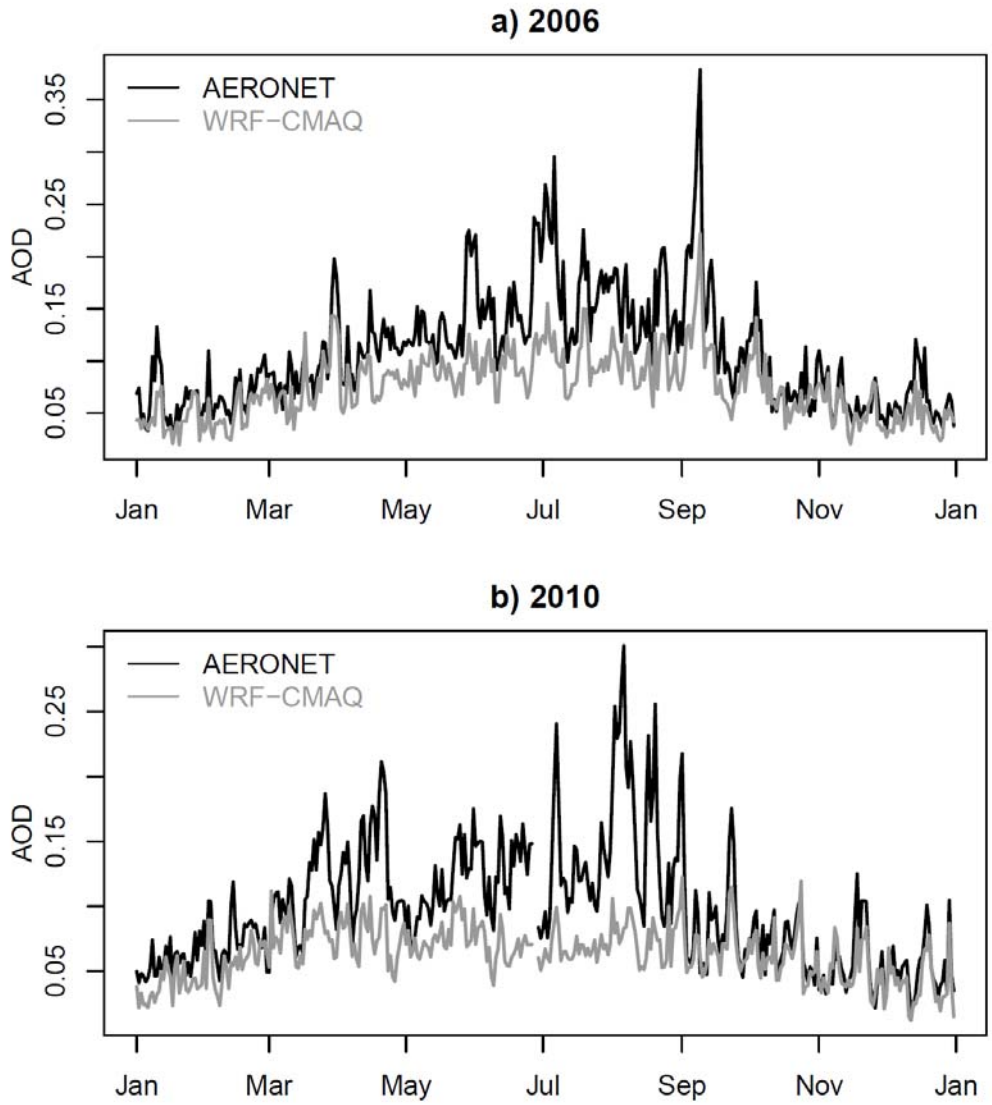

Figure 2: Time series of observed and modeled daily 500nm AOD spatially averaged across all AERONET sites in the modeling domain. a) 2006 and b) 2010.

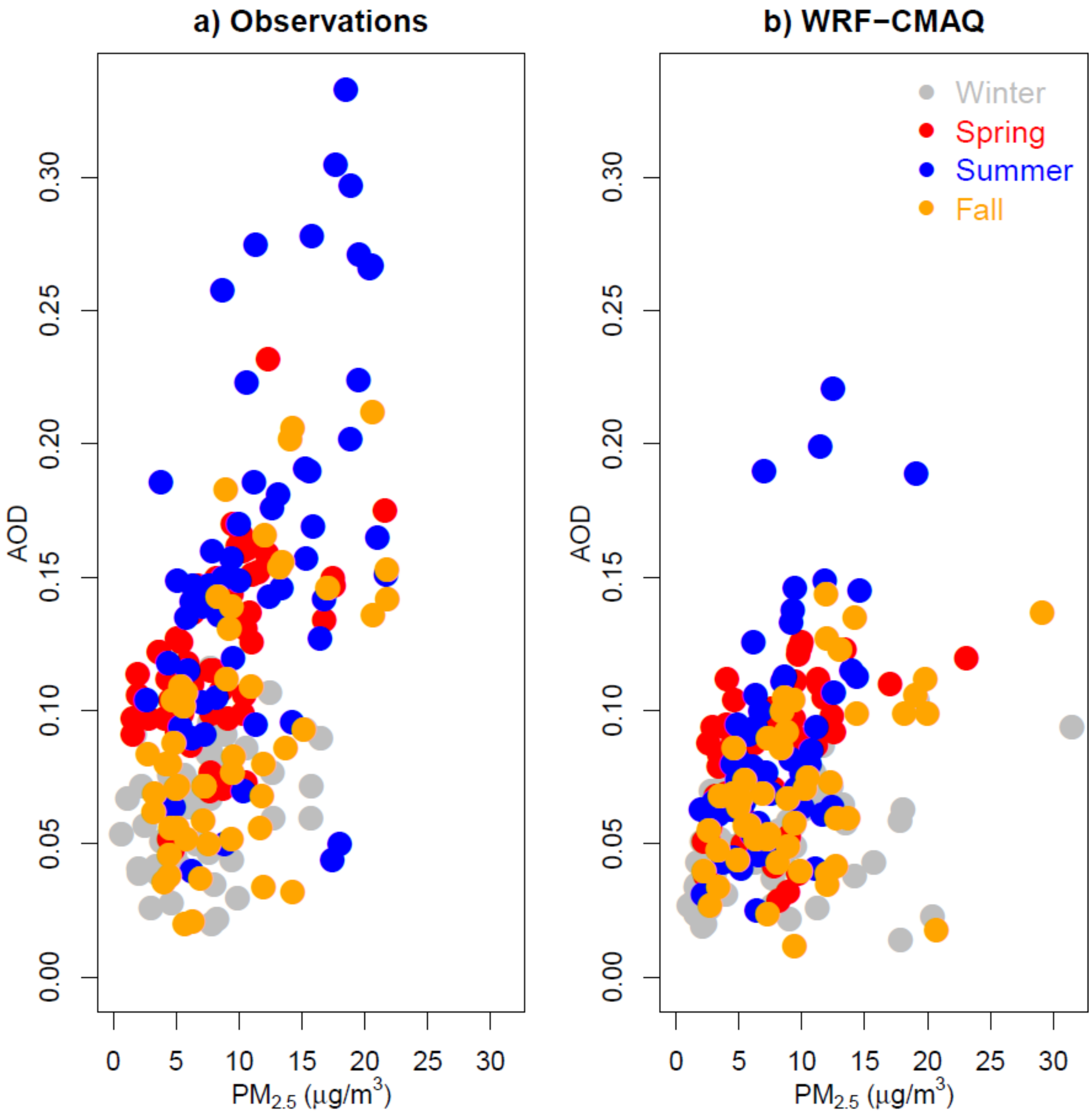

Figure 3: Scatterplot of quarterly average 500nm AOD and $PM_{2.5}$ concentrations derived from hourly observations and model values as described in the text. a) observations, b) model values. Both 2006 and 2010 values were used in this analysis. Each dot represents a pair of AOD/$PM_{2.5}$ monitoring sites or corresponding model grid cells.

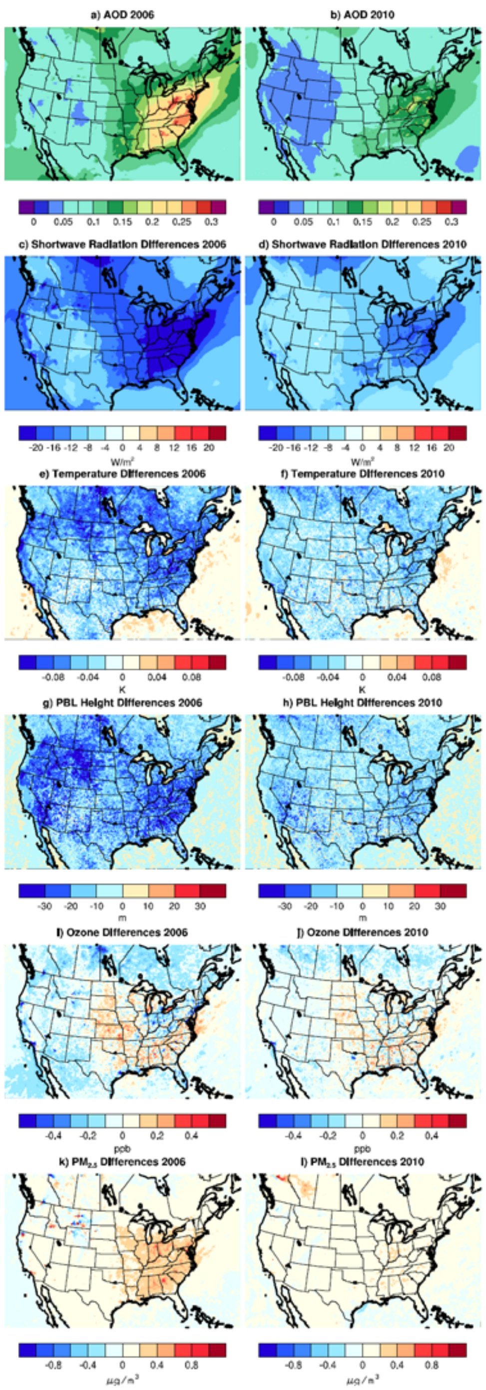

Figure 4: Top row: Average June – August daytime model simulated AOD for 2006 (left) and 2010 (right). Rows 2 – 6: differences in model simulated clear-sky short-wave radiation at the surface, 2m temperature, PBL height, ozone concentrations, and $PM_{2.5}$ concentrations between the WRF-CMAQ simulations with and without direct feedback effects. Results on the left are for 2006 and results on the right are for 2010. The differences were calculated over all June – August daytime hours

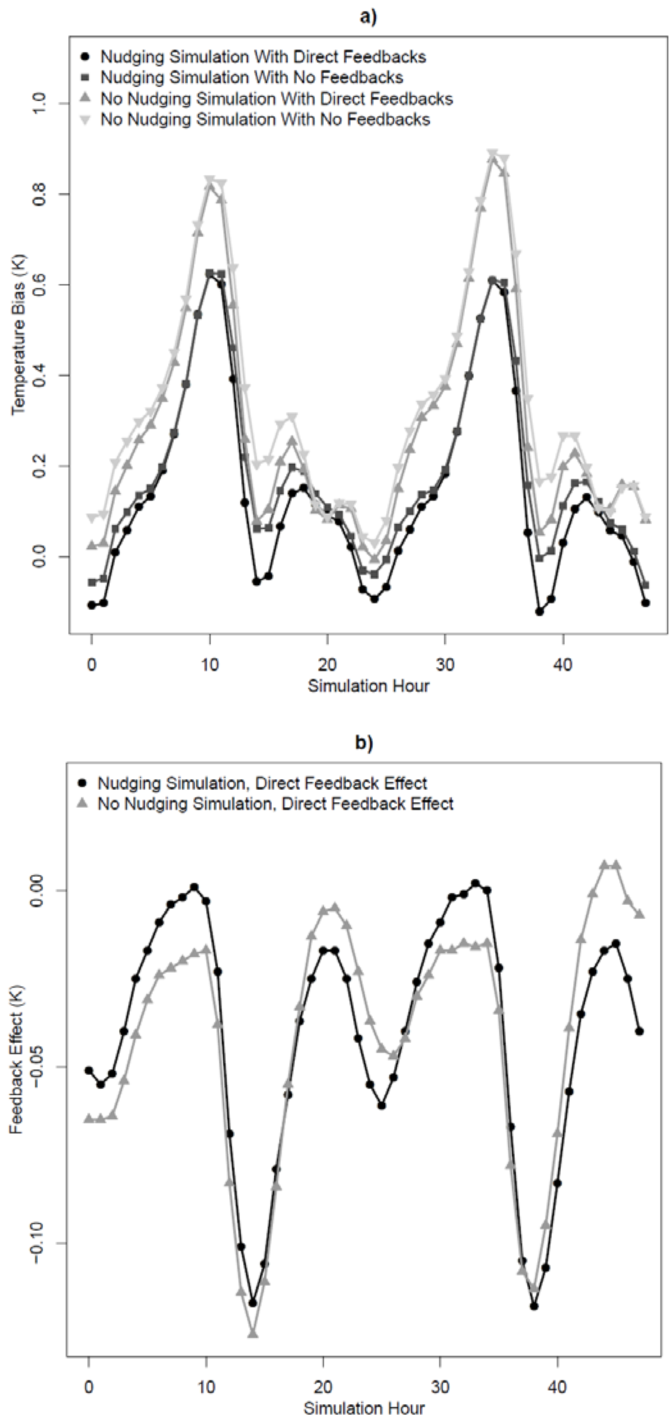

Figure 5: a) Time series of 2m temperature bias for the feedback and no feedback simulations performed with and without nudging as explained in the text. b) time series of differences between the feedback and no feedback simulations for both the nudging and no nudging model configurations.

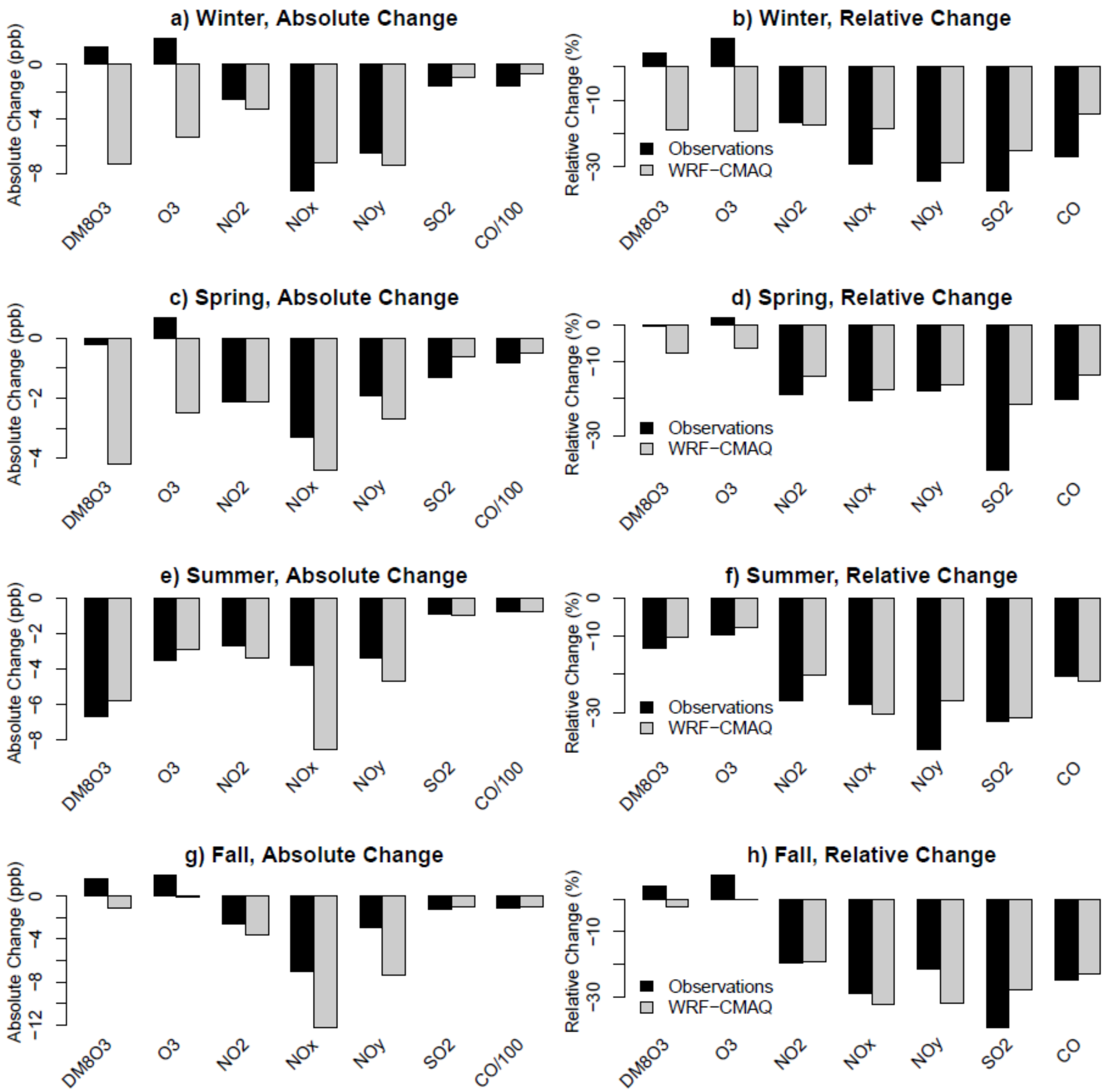

Figure 6: Observed (black) and simulated (grey) differences in quarterly average concentrations of several gas phase species observed at AQS monitors between 2010 and 2006. Absolute changes are shown on the left while relative changes are shown on the right. Absolute changes for CO have been divided by 100 to be accommodated on the same vertical scale.

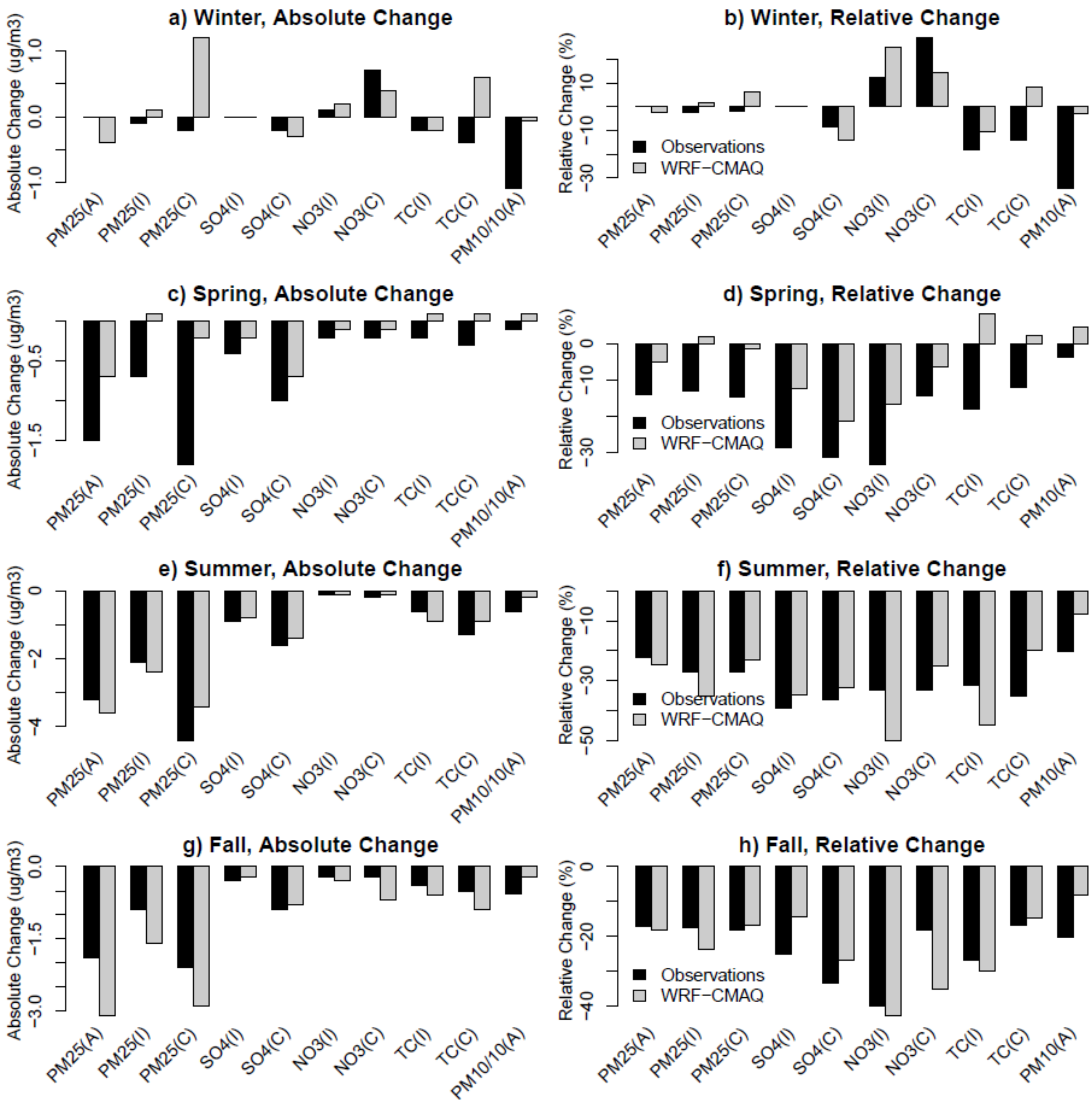

Figure 7: As in Figure 6 but for $PM_{2.5}$ total mass, select $PM_{2.5}$ species, and PM_{10} total mass. Absolute changes for PM_{10} have been divided by 10 to be accommodated on the same vertical scale. Letters in parenthesis indicate the monitoring network: A – AQS, I – IMPROVE, C - CSN.

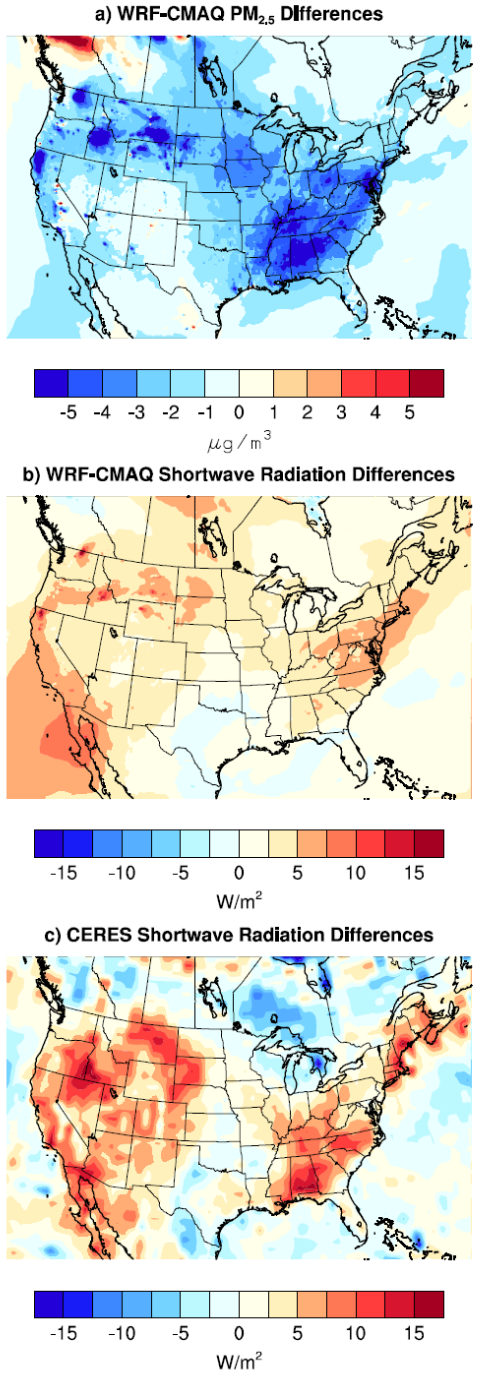

Figure 8: a) Differences in model simulated $PM_{2.5}$ concentrations between 2010 and 2006 averaged over all June – August daytime hours. b) as in a) but for clear-sky short-wave radiation at the surface. c) as in b) but for CERES satellite observations rather than WRF-CMAQ model simulations.

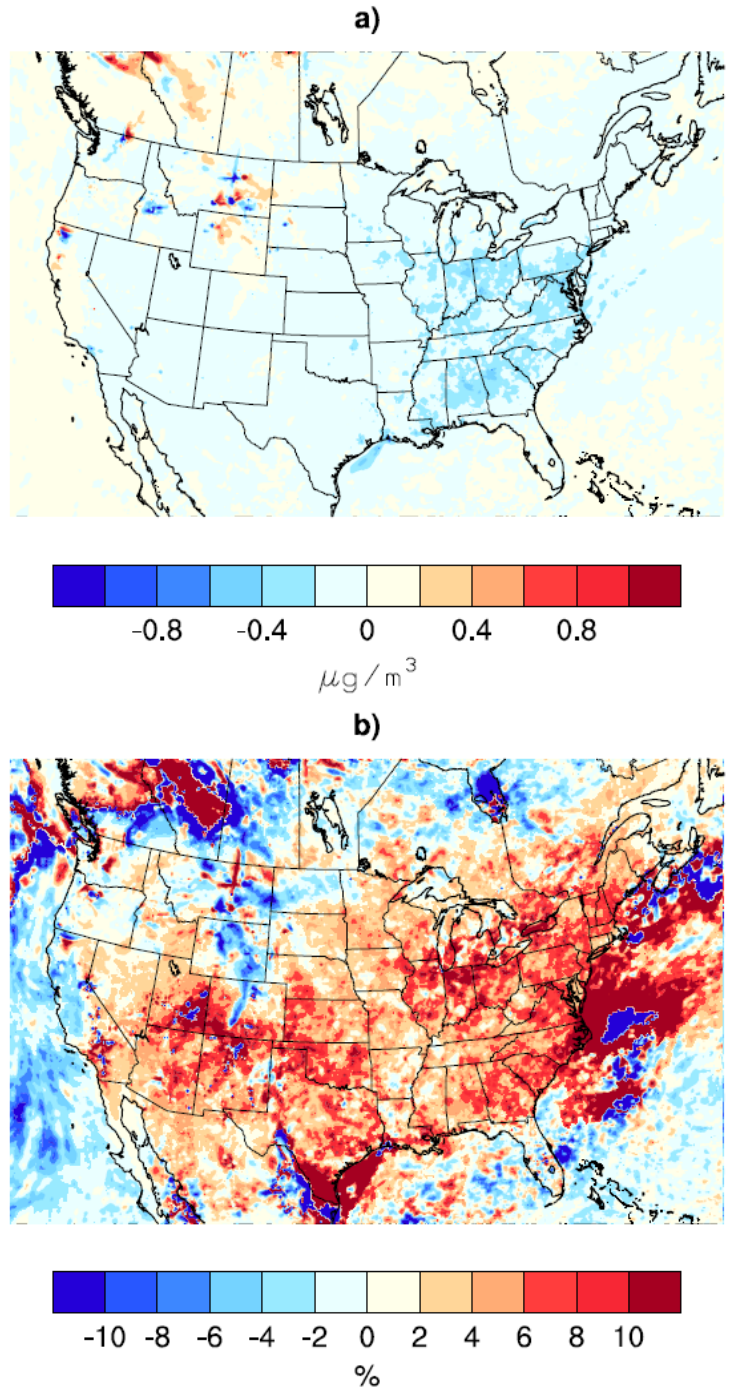

Figure 9: a) Differences in 2010-2006 changes of June – August daytime average $PM_{2.5}$ concentrations between the feedback and no feedback configurations of the WRF-CMAQ modeling system. Blue colors indicate areas where the feedback configuration simulated greater reductions (or smaller increases) between 2010 and 2006 than the no feedback configuration, while the opposite holds true for the areas indicated in red. b) as in a) but normalized by the 2010-2006 change simulated by the no feedback configuration and converted to a percentage scale.